Maritime component in aerosol optical models derived from Aerosol Robotic Network data

A. Smirnov,[1,2] B. N. Holben,[2] O. Dubovik,[1,2] R. Frouin,[3] T. F. Eck,[1,2] and I. Slutsker[2,4]

[1] Aerosol optical properties above the oceans vary considerably, depending on contributions of major aerosol components, i.e., urban/industrial pollution, desert dust, biomass burning, and maritime. The optical characterization of these aerosols is fundamental to the parameterization of radiative forcing models as well as to the atmospheric correction of ocean color imagery. We present a model of the maritime aerosol component derived using Aerosol Robotic Network (AERONET) data from three island locations: Bermuda (Atlantic Ocean), Lanai, Hawaii (Pacific Ocean), and Kaashidhoo, Maldives (Indian Ocean). To retrieve the maritime component, we have considered the data set with aerosol optical depth at a wavelength 500 nm less than 0.15 and Angstrom parameter α less than 1. The inferred maritime component in the columnar size distribution, which was found to be very similar for the three study sites, is bimodal with a fine mode at an effective radius (r_{eff}) $\sim 0.11-0.14$ μm and a coarse mode r_{eff} of $\sim 1.8-2.1$ μm. The results are comparable with size distributions reported in the literature. The refractive index is spectrally independent and estimated to be 1.37-0.001i (single-scattering albedo is about 0.98), based on the single-component homogenous particle composition assumption. Fractional contributions of the fine and coarse modes to the computed τ_a (500 nm) are within the range of $\tau_{fine} \sim 0.03-0.05$ and $\tau_{coarse} \sim 0.05-0.06$ correspondingly. Angstrom parameters vary from ~ 0.8 to 1.0 computed in the UV-visible (340–670 nm) and from 0.4 to 0.5 estimated in the near IR (870–2130 nm) spectral ranges. Aerosol phase functions are very similar for all three sites considered. The maritime aerosol component presented in this paper can serve as a candidate model in atmospheric correction algorithms. *INDEX TERMS:* 0305 Atmospheric Composition and Structure: Aerosols and particles (0345, 4801); 0360 Atmospheric Composition and Structure: Transmission and scattering of radiation; 1640 Global Change: Remote sensing; 4548 Oceanography: Physical: Ocean fog and aerosols; 4801 Oceanography: Biological and Chemical: Aerosols (0305); *KEYWORDS:* aerosol optical depth, Sun photometer, maritime aerosol, atmospheric correction, retrieval, phase function

Citation: Smirnov, A., B. N. Holben, O. Dubovik, R. Frouin, T. F. Eck, and I. Slutsker, Maritime component in aerosol optical models derived from Aerosol Robotic Network data, *J. Geophys. Res.*, *108*(D1), 4033, doi:10.1029/2002JD002701, 2003.

1. Introduction

[2] The quality of bio-optical products of satellite ocean color sensors is strongly dependent on the accuracy of atmospheric correction algorithms. Aerosol optical properties over the oceans vary considerably. In order to simulate aerosol optical conditions over the oceans major aerosol types should be considered: urban/industrial pollution, pure oceanic air, biomass burning aerosol and desert dust. The maritime aerosol component is important for every atmos-

pheric correction algorithm [see, e.g., *Badaev et al.*, 1989; *Fraser et al.*, 1997; *Gordon and Wang*, 1994; *Gordon*, 1997; *Chomko and Gordon*, 1998; *Gao et al.*, 2000]. Currently an oceanic aerosol model of *Shettle and Fenn* [1979] is widely used to account for the atmospheric aerosol contribution to the satellite-measured radiance. Verification of aerosol models for satellite ocean color remote sensing was attempted by *Schwindling et al.* [1998]. Based on the limited atmospheric optical measurements they concluded that, within measurement accuracy, the Shettle-Fenn model fits the observations.

[3] In the last decade significant experimental data was collected over the oceans by AERONET (Aerosol Robotic Network) radiometers, mainly, however, from island sites [*Holben et al.*, 2001; *Eck et al.*, 2001; *Smirnov et al.*, 2002]. This database of known quality (calibration is easily traceable, data are in the public domain and accessible virtually from everywhere via Internet, computations are reproducible, etc. [*Holben et al.*, 1998]) allows the estimation of a

[1]Goddard Earth Sciences and Technology Center, University of Maryland, Baltimore County, Baltimore, Maryland, USA.
[2]Biospheric Sciences Branch, NASA Goddard Space Flight Center, Greenbelt, Maryland, USA.
[3]Scripps Institution of Oceanography, La Jolla, California, USA.
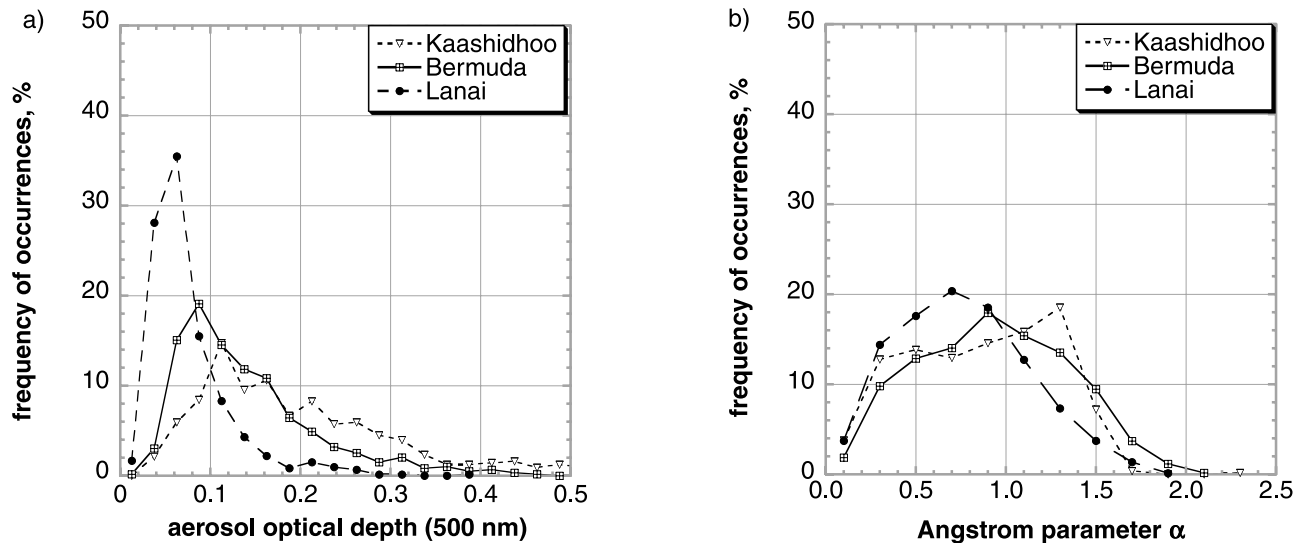[4]Science Systems and Applications, Inc., Lanham, Maryland, USA.

Figure 1. Frequency of occurrences of aerosol optical depth at 500 nm (a) and Angstrom parameter (b) for Lanai, Bermuda and Kaashidhoo.

number of candidate aerosol models and, perhaps, better aerosol modeling in the atmospheric correction of ocean color imagery.

[4] In the current study we consider primarily pure oceanic air. To retrieve a "pure maritime" component we will consider the data set with the aerosol optical depth smaller than 0.15 at a wavelength 500 nm and Angstrom parameter α less than 1 (α is a parameter in the following approximation: $\tau_a \sim \lambda^{-\alpha}$). The aerosol optical model includes information about optical parameters (aerosol optical depth and its spectral dependence, phase function and single-scattering albedo) and microphysical characteristics (size distribution and its parameters, refractive index).

2. Analysis

[5] AERONET is a federated international network of sun/sky radiometers. AERONET has existed since 1993 and maintains more than 150 automatic instruments (sun/sky radiometers) worldwide [*Holben et al.*, 1998, 2001]. Data are publicly available online in near real-time mode (http://aeronet.gsfc.nasa.gov). All of the measurements reported in this paper were made with the automatic Sun and sky scanning radiometers CIMEL. Instrument description details are given by *Holben et al.* [1998]. We will briefly discuss some instrument characteristics below. *Holben et al.* [1998] and *Eck et al.* [1999] addressed instrumental uncertainties, following *Russell et al.* [1993]. An automated cloud-screening algorithm [*Smirnov et al.*, 2000] is applied to the direct sun measurements of τ_a. A flexible inversion algorithm, developed by *Dubovik and King* [2000], was used to retrieve columnar aerosol volume size distributions, refractive indices and single-scattering albedos from the direct sun and diffuse (solar almucantar) sky radiance measurements. *Dubovik et al.* [2000, 2002] studied the accuracy of the retrieved parameters in detail.

[6] The CIMEL Sun and sky radiometer measures direct sun radiance in the eight spectral channels between 340 and 1020 nm (340, 380, 440, 500, 670, 870, 940 and 1020 nm).

The 940 nm data is used for the columnar water vapor content estimations. Diffuse sky radiances in the solar almucantar are acquired at 440, 670, 870 and 1020 nm wavelengths. The spectral dependence of aerosol optical depth $\tau_a(\lambda)$ is characterized by the Angstrom parameter α, derived from a multi-spectral log-linear fit to the classical equation $\tau_a \sim \lambda^{-\alpha}$ (based on the 4 CIMEL wavelengths in the range 440–870 nm unless otherwise stated). Typical total uncertainty in $\tau_a(\lambda)$ for a field instrument is ±0.01–0.02 and is spectrally dependent with the higher errors (±0.02) in the UV spectral range [*Eck et al.*, 1999].

[7] AERONET has accumulated a significant amount of data at operational sites in the Pacific (Lanai, Hawaii), in the Atlantic (Bermuda) and in the Indian Ocean (Kaashidhoo, Maldives). Detailed information on the seasonal, inter- and intra-annual variability of aerosol optical properties for those sites can be found in the studies by *Holben et al.* [2001], *Eck et al.* [2001], and *Smirnov et al.* [2002].

[8] Figures 1a and 1b present the frequency of occurrence distributions for the daily averaged τ_a(500 nm) and α. The frequency distribution for Lanai (Pacific Ocean) shows that the vast majority of optical depths are less than 0.10. The mode is situated at about 0.06. The distribution is relatively broad for Bermuda with a modal value of 0.09. Measurements over the Maldives (Kaashidhoo) show a notable seasonality with a significant aerosol loading during the NE monsoon months [*Eck et al.*, 2001]. The modal τ_a(500 nm) value at this site is about 0.11, however the distribution is much wider with only 40% of τ_a(500 nm) smaller than 0.15. The Angstrom parameter frequency distribution has a maximum at 1.3 for Kaashidhoo, peaks at 0.9 for Bermuda, and is skewed towards smaller $\alpha \sim 0.7$ for Lanai.

[9] In order to retrieve a "pure maritime" component we limited our analysis to aerosol optical depths at 500 nm smaller than 0.15 and Angstrom parameters less than 1. This choice is based on the following considerations. Summary of aerosol optical depth measurements in maritime and coastal areas [*Smirnov et al.*, 2002] indicate, generally, a more transparent atmosphere (small aerosol concentrations)
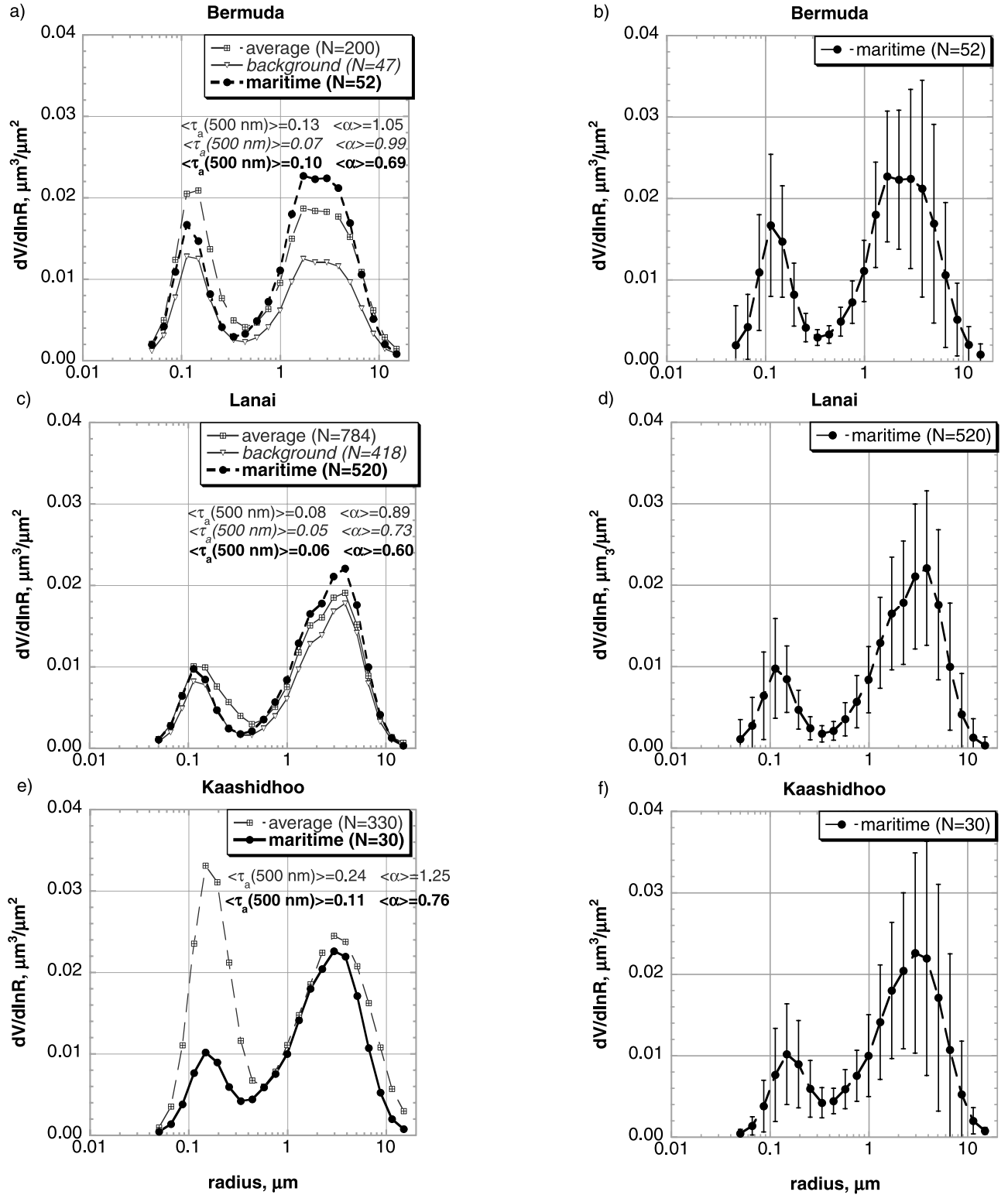
Figure 2. Average aerosol volume size distributions in the total column for Bermuda (a, b), Lanai (c, d), and Kaashidhoo (e, f). Vertical error bars show plus or minus one standard deviation of the average value.

over the Pacific Ocean as compared to the Atlantic and Indian Ocean. The spectral dependence of $\tau_a(\lambda)$ above the Pacific Ocean is more neutral than in the regions affected by continental sources, owing to a large fraction of coarse-mode aerosol of sea origin (sea-salt) in the size distribution. AERONET has four island sites in the remote tropical

Pacific Ocean (Midway, Lanai, Nauru and Tahiti). Statistics presented by *Smirnov et al.* [2002] for the Pacific sites and new data from Midway Island demonstrate that the majority of $\tau_a(500 \text{ nm})$ and α values (85%–99% and 75–97% correspondingly) are smaller than 0.15 and less than 1.0 respectively. Among several island sites in the Pacific we

have chosen only Lanai for our consideration simply because it has a reliable long-term record [*Holben et al.*, 2001; *Smirnov et al.*, 2002].

[10] Aerosol volume size distributions in the total column were retrieved from sun and sky radiance measurements according to *Dubovik and King* [2000] and *Dubovik et al.* [2000]. Retrieval errors in dV/dlnR do not exceed 15% for water-soluble aerosol type within the $0.1-7$ μm range, raising up to 80–100% for the sizes less than 0.1 μm and higher than 7 μm. The residual error threshold was less than or equal to 5% (between computed and measured radiances) and the number of scattering angles in the measured sky radiance distributions was not less than 21 [*Dubovik et al.*, 2002]. The same dataset was used for Bermuda and Lanai as in the paper by *Smirnov et al.* [2002].

[11] For the Bermuda dataset only 52 size distribution retrievals from 35 days correspond to the "pure maritime" conditions (τ_a(500 nm) < 0.15 and α < 1.0). Figure 2a presents "climatological average" (when all τ_a and α data are averaged) from *Smirnov et al.* [2002], "background average" (for conditions that correspond to the baseline optical depth, defined as the median for periods of stable (standard deviation <0.02) optical depth during $2-6$ days, according to *Kaufman et al.* [2001]), and the "maritime" average, for the maritime aerosol discrimination criteria defined above. The number of averaged retrievals is shown in parentheses. Variability of the "maritime" size distribution can be seen in Figure 2b where the vertical error bars show one standard deviation from the average value. The volume fraction of fine particles is higher for the "climatological average" due to advection from North America. Coarse particles account for almost 75% of the "maritime" volume concentration. Baseline maritime conditions over Bermuda correspond to the lowest columnar volume concentration in Figure 2a.

[12] The air over Lanai is primarily "truly maritime", however, long-range high-altitude dust transport from Asia

Table 1. Aerosol Volume Size Distributions and Their Parameters[a]

	dV/dlnR, μm^3/μm^2		
R, μm	Lanai	Bermuda	Kaashidhoo
0.050	1.08E-03	1.97E-03	4.70E-04
0.066	2.77E-03	4.23E-03	1.39E-03
0.086	6.42E-03	1.09E-02	3.82E-03
0.113	9.77E-03	1.67E-02	7.65E-03
0.148	8.46E-03	1.47E-02	1.02E-02
0.194	4.70E-03	8.20E-03	8.96E-03
0.255	2.44E-03	4.15E-03	5.95E-03
0.335	1.76E-03	2.93E-03	4.23E-03
0.439	2.11E-03	3.31E-03	4.44E-03
0.576	3.54E-03	4.87E-03	5.89E-03
0.756	5.69E-03	7.26E-03	7.54E-03
0.992	8.40E-03	1.11E-02	1.00E-02
1.302	1.29E-02	1.80E-02	1.41E-02
1.708	1.65E-02	2.27E-02	1.80E-02
2.241	1.79E-02	2.23E-02	2.04E-02
2.940	2.11E-02	2.24E-02	2.26E-02
3.857	2.21E-02	2.12E-02	2.20E-02
5.061	1.76E-02	1.69E-02	1.71E-02
6.641	9.98E-03	1.06E-02	1.07E-02
8.713	4.13E-03	5.13E-03	5.25E-03
11.432	1.28E-03	2.04E-03	2.01E-03
15.000	3.36E-04	8.23E-04	7.83E-04
C_v, fine	0.010	0.017	0.012
R_v, fine	0.123	0.124	0.164
R_{eff}, fine	0.113	0.114	0.146
σ, fine	0.42	0.41	0.48
C_v, coarse	0.039	0.047	0.044
R_v, coarse	2.78	2.44	2.62
R_{eff}, coarse	2.13	1.81	1.92
σ, coarse	0.73	0.77	0.79
N	520	52	30

[a]C_v is the columnar volume of particles per unit cross section of atmospheric column (μm^3/μm^2), R_v is the volume geometric mean radius (μm), Reff is the effective radius (μm), σ is the geometric standard deviation, and N is the number of averaged retrievals.
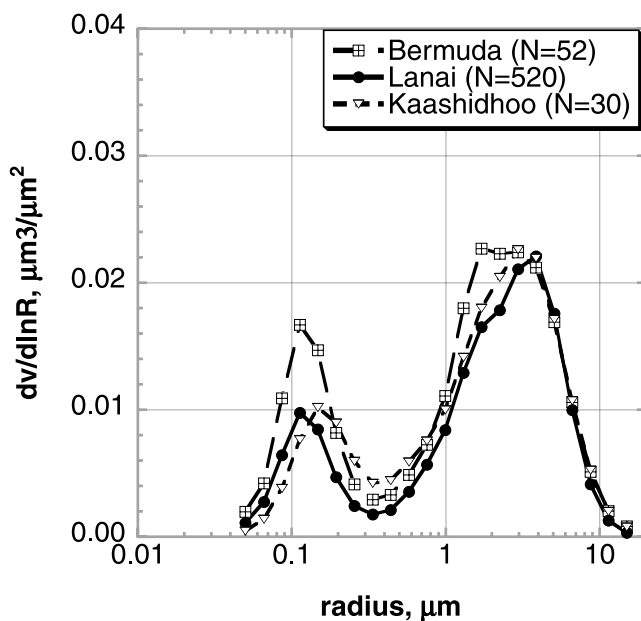
in the spring season months [*Shaw*, 1980; *Perry et al.*, 1999; *Thulasiraman et al.*, 2002] can elevate daily and monthly averages [*Holben et al.*, 2001]. Figure 2c shows, that in fact, there is almost no difference between the "climatological average" (consists of N = 784 averaged retrievals) and "maritime" average (N = 520). As expected, baseline (or background) conditions [*Kaufman et al.*, 2001] yielded the smallest columnar concentration. Vertical error bars (Figure 2d) are even smaller than in Figure 2b, indicating less variability for the Lanai size distributions.

[13] As we previously noted, aerosol loading over the Maldives (Kaashidhoo) demonstrates inter- and intra-annual variability and seasonality depending on the contribution of various aerosol species [*Satheesh et al.*, 1999; *Ramanathan et al.*, 2001]. For the whole analyzing period (from February 1998 through October 2000) 330 retrievals satisfied the 5% residual error and 21 scattering angle criteria. Only 30 retrievals from 22 days were averaged for our "maritime" conditions. Despite the fact that there is always a possibility of some residual dust aerosol contamination, we believe it is minimal, since the residual error for such cases should be higher than 5% because of particle non-sphericity [*Dubovik et al.*, 2002]. Figures 2e and 2f present averaged volume size distributions for Kaashidhoo. Variability of the coarse fraction is slightly higher than for the other two sites considered.

[14] Figure 3 and Table 1 summarize particle size distribution results for our maritime criteria. They reveal a lot of
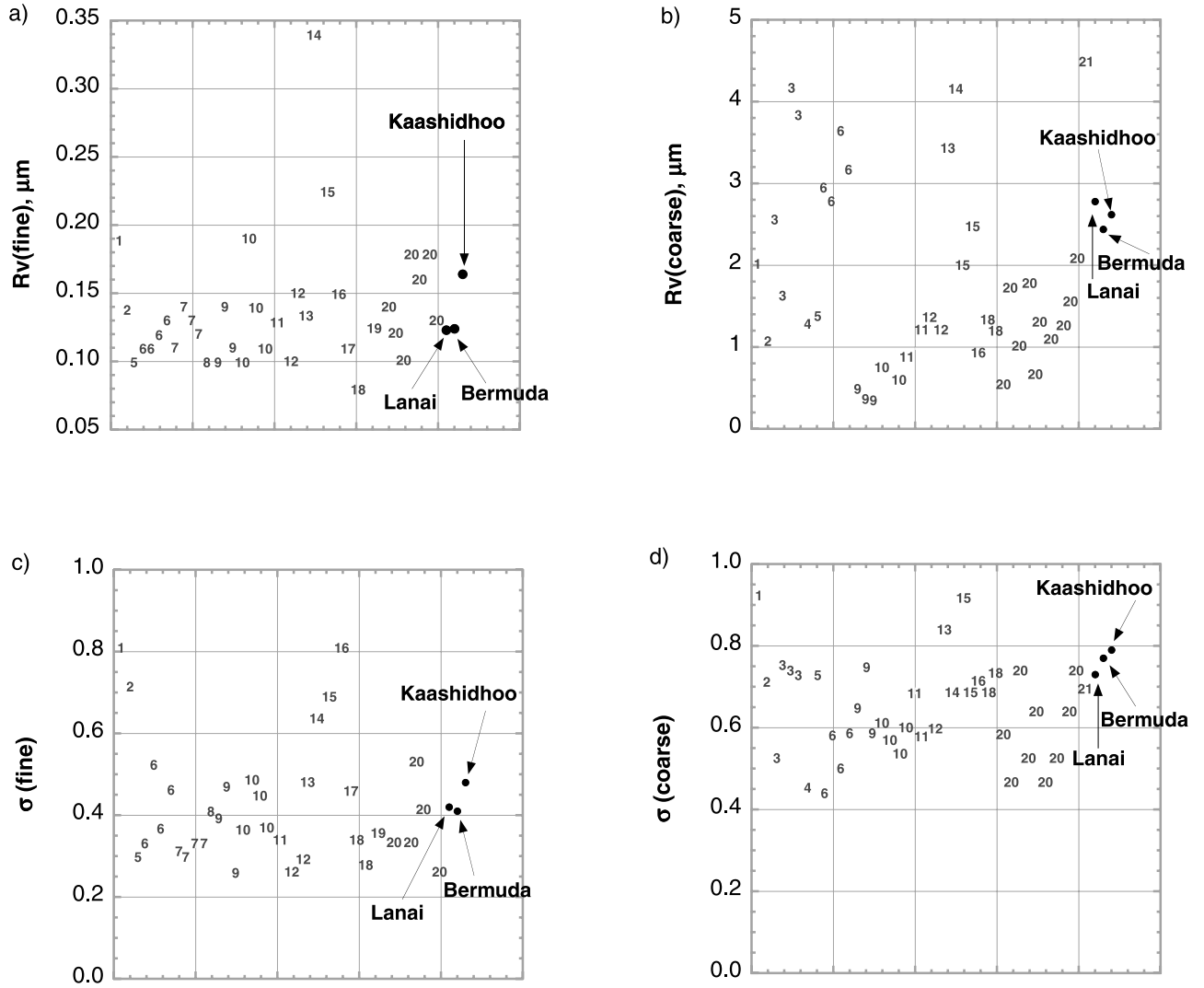

Figure 3. Maritime components of the columnar volume size distributions for Bermuda, Lanai and Kaashidhoo.

Figure 4. Comparison of aerosol size distribution parameters from literature sources (Table 2 of *Smirnov et al.* [2002]) to those derived in the current study. The volume geometric mean radii for the fine (a) and coarse (b) modes, and corresponding geometric standard deviations (c and d) are presented consecutively as given by *Smirnov et al.* [2002, Table 2]; that is, 1, *Shettle and Fenn* [1979]; 2, *Gathman* [1983]; 3, *Horvath et al.* [1990]; 4, *Patterson et al.* [1980]; 5, *Jennings and O'Dowd* [1990]; 6, *Kim et al.* [1990]; 7, *O'Dowd et al.* [1993]; 8, *Pueschel et al.* [1994]; 9, *Kim et al.* [1995]; 10, *Gras* [1995]; 11, *Quinn et al.* [1995]; 12, *Quinn et al.* [1996]; 13, *Porter and Clarke* [1997]; 14, *O'Dowd et al.* [1997]; 15, *Jennings et al.* [1997]; 16, *Hess et al.* [1998]; 17, *Brechtel et al.* [1998]; 18, *Bates et al.* [1998]; 19, *Bates et al.* [2000]; 20, *Quinn et al.* [2001]; 21, *Reid et al.* [2001].

similarity among "maritime" averaged columnar volume size distributions for Bermuda, Lanai and Kaashidhoo. The amplitudes of the coarse mode are very close. The fine mode geometric mean radius for Kaashidhoo is higher by ~25% compared to Lanai. This result could be at least partly attributable to higher precipitable water amount and subsequent hygroscopic particle growth. Computed averaged water vapor content values are 2.79 cm, 2.87 cm and 4.34 cm for Bermuda, Lanai and Kaashidhoo correspondingly.

[15] For each mode the lognormal distribution is defined as:

$$\frac{dV}{d\ln R} = \frac{C_v}{\sigma\sqrt{2\pi}} \exp\left(-\frac{1}{2}\left(\frac{\ln(R/R_v)}{\sigma}\right)^2\right)$$

where $dV/d\ln R$ is the volume size distribution, C_v is the columnar volume of particles per unit cross section of atmospheric column ($\mu m^3/\mu m^2$), R_v is the volume geometric mean radius (μm), and σ is the geometric standard deviation.

[16] Parameters of the lognormal fits are not inconsistent with previous studies (see summary given by *Smirnov et al.* [2002]). Direct comparison with the in situ size distributions is shown in Figure 4. The x axis of all the Figure 4 graphs is simply an arbitrary counting index used to better display the different data sets. Figures 4a to 4d show respectively the volume geometric mean radii for the fine and coarse fractions and corresponding geometric standard deviations from the literature sources (Table 2 of *Smirnov et al.* [2002]) and the lognormal parameters listed in Table 1 (of this

Table 2. Aerosol Spectral Phase Function, Average Cosine, Aerosol Optical Depth, and Single-Scattering Albedo Computed Using Size Distribution Over Lanai and Refractive Index of 1.37-0.001i

Scattering Angle	340 nm	380 nm	440 nm	500 nm	670 nm	870 nm	1020 nm	1240 nm	1650 nm	2130 nm
0.00	325.639	296.391	259.882	229.214	164.352	116.957	94.533	72.218	50.444	37.930
1.00	200.001	196.523	188.067	176.684	141.000	106.600	88.383	69.043	49.199	37.370
1.73	117.511	121.560	124.742	124.115	111.235	91.148	78.526	63.609	46.928	36.311
2.60	68.704	72.913	78.229	81.277	81.045	72.534	65.497	55.709	43.267	34.497
3.46	45.597	48.707	53.116	56.308	59.894	57.346	53.921	47.980	39.226	32.328
4.33	32.877	35.144	38.546	41.244	45.485	45.642	44.330	41.031	35.175	29.964
5.20	25.202	26.874	29.511	31.757	35.758	37.000	36.802	35.158	31.413	27.594
6.06	20.279	21.501	23.568	25.453	29.060	30.687	31.038	30.371	28.073	25.342
6.93	16.908	17.768	19.362	20.951	24.166	25.897	26.513	26.417	25.101	23.210
8.66	12.889	13.227	14.099	15.185	17.705	19.385	20.175	20.573	20.307	19.483
10.39	10.655	10.677	11.084	11.765	13.670	15.203	16.003	16.547	16.714	16.432
12.12	9.220	9.056	9.192	9.586	10.971	12.314	13.057	13.635	13.984	13.964
13.85	8.188	7.925	7.895	8.105	9.082	10.208	10.867	11.432	11.861	11.965
15.57	7.387	7.080	6.940	7.028	7.709	8.624	9.182	9.714	10.174	10.338
17.30	6.724	6.402	6.180	6.187	6.655	7.379	7.838	8.320	8.787	8.980
21.61	5.402	5.108	4.820	4.707	4.843	5.218	5.492	5.805	6.222	6.440
25.90	4.372	4.133	3.865	3.698	3.649	3.839	3.990	4.168	4.481	4.694
30.19	3.517	3.350	3.126	2.964	2.814	2.888	2.958	3.061	3.268	3.454
34.46	2.807	2.706	2.534	2.394	2.201	2.202	2.231	2.288	2.415	2.563
38.71	2.232	2.177	2.059	1.941	1.742	1.697	1.705	1.732	1.809	1.918
42.94	1.769	1.746	1.674	1.581	1.397	1.326	1.318	1.327	1.375	1.452
51.32	1.110	1.125	1.105	1.060	0.923	0.839	0.814	0.813	0.830	0.864
59.57	0.707	0.731	0.737	0.717	0.628	0.556	0.529	0.520	0.525	0.543
67.65	0.462	0.487	0.501	0.496	0.443	0.387	0.361	0.352	0.352	0.362
75.52	0.313	0.335	0.351	0.353	0.323	0.282	0.262	0.251	0.249	0.255
83.12	0.223	0.240	0.257	0.261	0.246	0.216	0.199	0.190	0.186	0.189
97.18	0.135	0.146	0.159	0.168	0.168	0.152	0.139	0.131	0.125	0.126
108.94	0.103	0.112	0.124	0.133	0.140	0.129	0.119	0.111	0.103	0.103
117.05	0.092	0.100	0.112	0.122	0.133	0.124	0.115	0.107	0.099	0.098
120.00	0.090	0.098	0.110	0.120	0.132	0.125	0.115	0.107	0.099	0.098
130.00	0.091	0.099	0.113	0.124	0.141	0.137	0.127	0.119	0.109	0.107
147.50	0.162	0.176	0.196	0.213	0.236	0.227	0.212	0.196	0.174	0.159
154.30	0.172	0.189	0.214	0.235	0.265	0.262	0.249	0.232	0.205	0.188
170.00	0.223	0.242	0.269	0.291	0.317	0.303	0.285	0.262	0.226	0.195
180.00	0.294	0.317	0.348	0.373	0.395	0.369	0.345	0.312	0.265	0.222
$\langle g \rangle$	0.742	0.729	0.716	0.707	0.706	0.722	0.734	0.748	0.761	0.763
τ_a	0.113	0.101	0.087	0.078	0.063	0.056	0.053	0.049	0.043	0.039
ω_0	0.977	0.976	0.976	0.976	0.977	0.980	0.982	0.984	0.987	0.988

paper) for Bermuda, Lanai and Kaashidhoo. It can be seen from Figure 4a that Rv(fine) from Table 1 agree well with almost all of the in situ measurement results. The coarse aerosol mode radius Rv(coarse) retrieved in the present study is not inconsistent with the in situ measurements, being, however, slightly higher than the majority, and close to the results of *Horvath et al.* [1990], *Kim et al.* [1990], and *Jennings et al.* [1997]. Overall, in situ data show a very wide range of results for Rv (coarse). Width parameters σ(fine) and σ(coarse) (Table 1) are in rather remarkable agreement especially for the fine fraction (Figure 4c). The fine aerosol mode is generally narrower than the coarse mode. The two most widely recognized models [*Shettle and Fenn*, 1979; *Gathman*, 1983] prescribe wider geometric standard deviations for the fine mode.

[17] There are, as yet, no published comparisons on the simultaneous in situ aerosol size distribution measurements (surface or aircraft) and columnar retrievals from AERONET radiometric measurements. Several comparisons, however, have recently been made. *Haywood et al.* [2003] reported a good agreement between aerosol spectra measured by integrated vertical profile PCASP and derived from the AERONET CIMEL during the SAFARI 2000 campaign for biomass burning aerosols at Etosha Pan, Namibia. *Eck et al.* [2003] compared the normalized fine mode biomass

burning aerosol lognormal size distribution from in situ measurements of local smoke in Cuiaba, Brazil [*Reid et al.*, 1998] with the lognormal Cerrado (Brazil) smoke model of *Dubovik et al.* [2002] and also found excellent agreement. A preliminary comparison of in situ measured size distributions at several altitudes from aircraft with the AERONET columnar retrieved values during INDOEX showed close similarities for the fine mode (S. Howell, personal communication, cited by *Eck et al.* [2001]). Fine mode volume size distribution comparisons proved to be in reasonable agreement for the EOPACE 1999 winter field campaign (J. Reid, personal communication, 1999) and for the PRIDE experiment [*Reid et al.*, 2003]. Coarse mode inversions from AERONET sun/sky data, however, were not always consistent with the columnar integrated size distributions measured with FSSP (EOPACE and PRIDE campaigns). *Reid et al.* [2003] reported that the inversions gave consistent average size distributions in the middle of the particle size ranges measured using the aerodynamic and optical particle counter methods.

[18] Generally speaking, we may or may not find agreement between columnar retrievals and in situ measurements. There are a variety of reasons for this, starting with the fact that measurements in the total column are quite different from the measurements in the local volume. AERONET
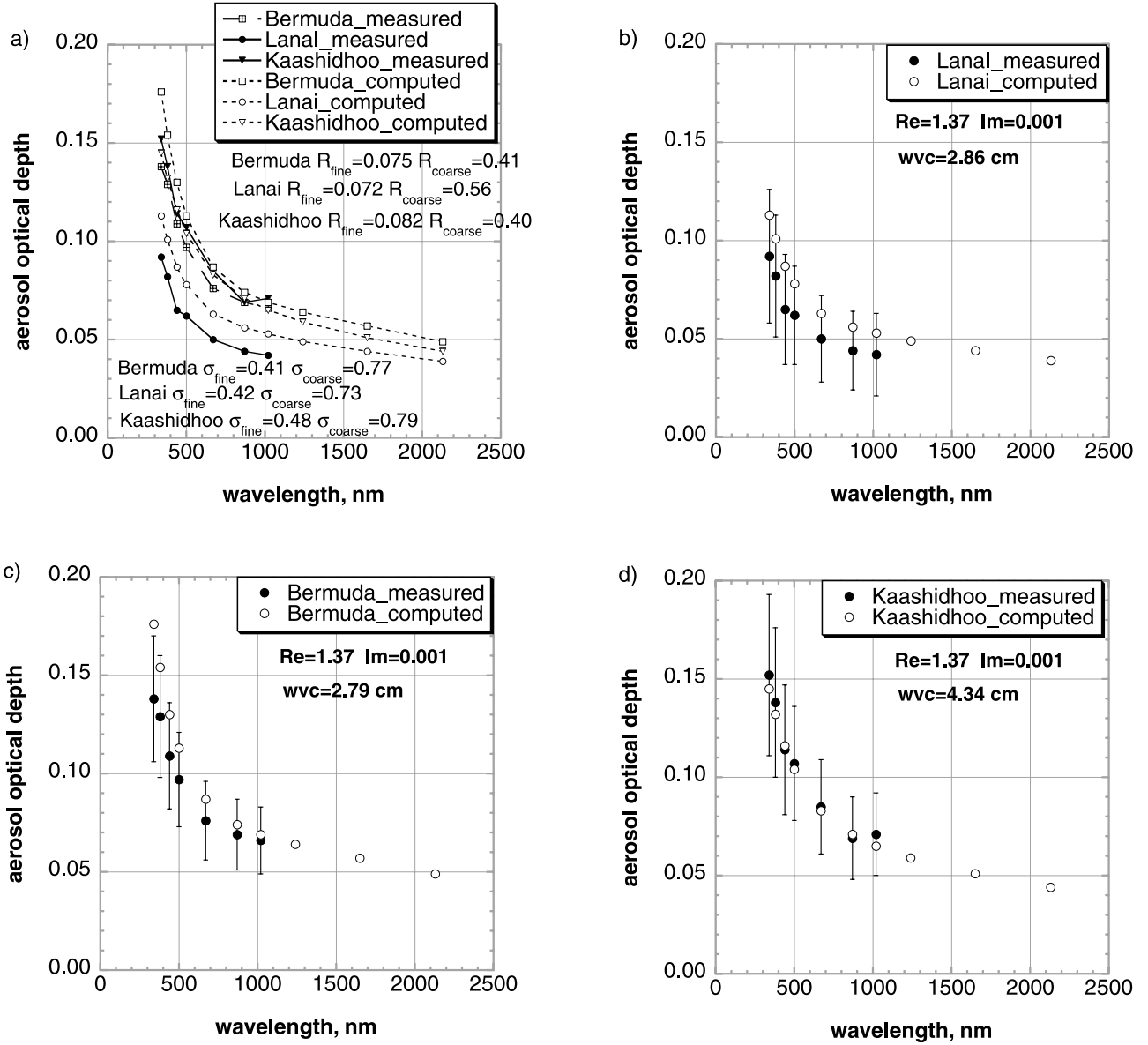
Figure 5. Comparison of spectral aerosol optical depths computed in the spectral range 340–2130 nm using size distributions from Figure 3 to the averaged $\tau_a(\lambda)$ measured in the range 340–1020 nm. Vertical error bars show plus or minus one standard deviation of the average measured value.

measures the aerosol scattering and absorption in its ambient state at the ambient relative humidity. It is not possible to make any humidity related adjustments, simply because the aerosol concentration profile and relative humidity profile are not known. The aerosol vertical profile is usually not known (except in the case of lidar or multi-altitude flights) and aerosol layers with different aerosol composition and species may exist. On the other hand methodological and instrumental biases of the in situ measurement technique [*Reid et al.*, 2003] inhibit direct comparisons of size distributions. The AERONET columnar retrievals that match sun and sky radiances within a known threshold of residual error are best considered as "optically equivalent" volume size distributions.

[19] *Dubovik et al.* [2000] pointed out, that errors in the retrieved refractive index of greater than 0.05 for the real part and 80–100% for the imaginary part should be expected when $\tau_a(440 \text{ nm})$ is relatively low (less than 0.20). Nevertheless, for our analysis we decided to employ the average refractive indices retrieved from the Lanai data set for computations at all three stations (see below). Simple averaging of all retrievals and all wavelengths (as given by *Dubovik et al.* [2002]) yielded 1.37 for the real part and 0.001 for the imaginary part of refractive index. Taken together, these values correspond to a single-scattering albedo value of 0.98.

[20] Our approach can be justified by the fact, that the Lanai data set is the biggest (N = 520) and the results obtained are more statistically robust. In their oceanic aerosol model, *Fraser et al.* [1997] chose an almost identical value (1.38 for the real part and 0.001 for the imaginary index to account for absorption by black carbon). The

method of *Dubovik and King* [2000] allows for the retrieval of only an "effective," single-component refractive index assuming, all particles are of homogenous composition. Recently, *Yan et al.* [2002] showed that the single-component approach might cause notable errors in atmospheric correction algorithms, especially for the absorbing aerosol and when relative humidity is high. However, for simplicity, we will use the values discussed above, noting, that the real part is close to the oceanic model of *Shettle and Fenn* [1979] (relative humidity ~80%) and the imaginary part is slightly lower than in their tropospheric model.

[21]   Figure 5 presents aerosol optical depths computed in the spectral range 340–2130 nm using average size distributions from Figure 3 and a refractive index of 1.37-0.001i, compared with the average of simultaneously measured $\tau_a(\lambda)$ in the 340–1020 nm spectral range constrained by the same maritime criteria discussed above. We also show parameters of the lognormal number size distributions, simply recomputed from the parameters listed in Table 1, and averaged columnar water vapor content (Figures 5b–5d). Figure 5a reflects general consistency among measured and calculated $\tau_a(\lambda)$, although the calculated τ_a is biased high versus measured τ_a for Lanai and Bermuda. Figures 5b–5d illustrate that the difference between measured and computed optical depths lies within one standard deviation for each site considered (vertical error bars on Figures 5b–5d show plus or minus one standard deviation from the average value), except for the 340 nm channel in the Bermuda case. Plotted standard deviations do not exceed 0.03 for Lanai and Bermuda, and are at most 0.04 for Kaashidhoo. We found the agreement between simulated and measured $\tau_a(\lambda)$ to be reasonable and accordingly we infer that a simply parameterized maritime model can be employed to characterize the optically equivalent maritime microphysical properties and associated aerosol optical depth. This approach is consistent with the sensitivity study of *Dubovik et al.* [2000], which showed that for the inversion
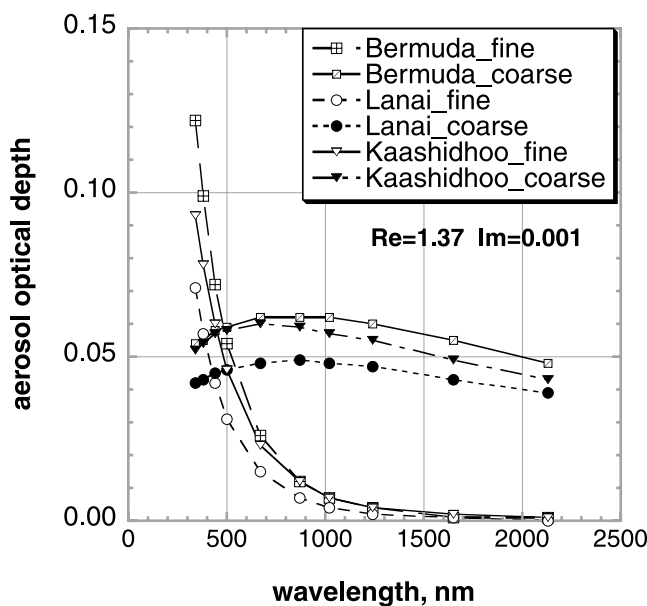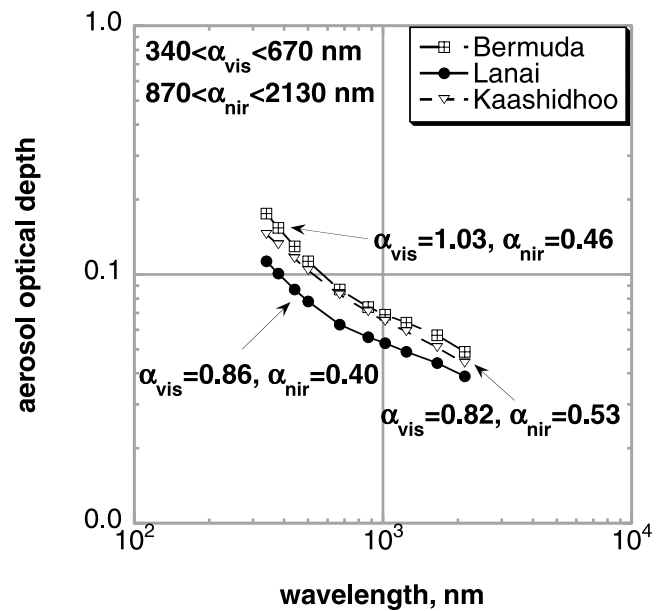

Figure 7.   Computed spectral aerosol optical depth and visible and near-IR Angstrom parameters.

scheme employed a single-component approach (with an "effective" refractive index) gives reasonable results.

[22]   We note that we did not achieve any better agreement between measured and calculated $\tau_a(\lambda)$ if a two-component approach was employed in the refractive index modeling. Specifically the application of the Shettle-Fenn oceanic model at a relative humidity of 80% for the coarse fraction and the Shettle-Fenn tropospheric model at the same relative humidity for the fine mode made the disagreement in the UV and blue spectral ranges even more pronounced.

[23]   Satellite measurements over the oceans [*Tanre et al.*, 1997] allow the retrieval of optical depth and its fine and coarse mode components. Computations of τ_{fine} and τ_{coarse} for the baseline oceanic conditions have been reported by *Kaufman et al.* [2001]. Here we present the estimations for the maritime aerosol component using size distributions from Table 1. The contribution of the fine and coarse modes is shown in Figure 6. The aerosol optical depth of the coarse fraction, being almost wavelength independent, is about 0.05–0.06. It is consistent with the experimental results of *Sakerin and Kabanov* [2002], who empirically separated the two aerosol components, and higher than τ_{coarse} for the baseline conditions [*Kaufman et al.*, 2001] by 0.02–0.03 or by a factor of 2. Spectral optical depth for the fine aerosol fraction is strongly spectrally dependent and also higher by a factor of 1.5 than τ_{fine} for the baseline conditions, We note as well that our τ_{fine} computations agrees favorably with the estimations of *Clarke et al.* [2001].

[24]   The computed aerosol optical depth spectral dependence has an inflection point around 670 nm (Figure 7). Fine particles mainly affect the UV and visible spectral ranges, while coarse particles dominate the optical depth variability in the IR and SWIR spectral ranges. We calculated the Angstrom parameter using a least squares method in two ranges: 340–670 nm (α_{vis}) and 870–2130 nm (α_{nir}). It can be seen (Figure 7) that the first parameter (α_{vis}) is higher by approximately factor of 2 or 0.5 in terms of $\Delta\alpha$. Based on

Figure 6.   Fine and coarse mode contributions to the computed spectral aerosol optical depths.
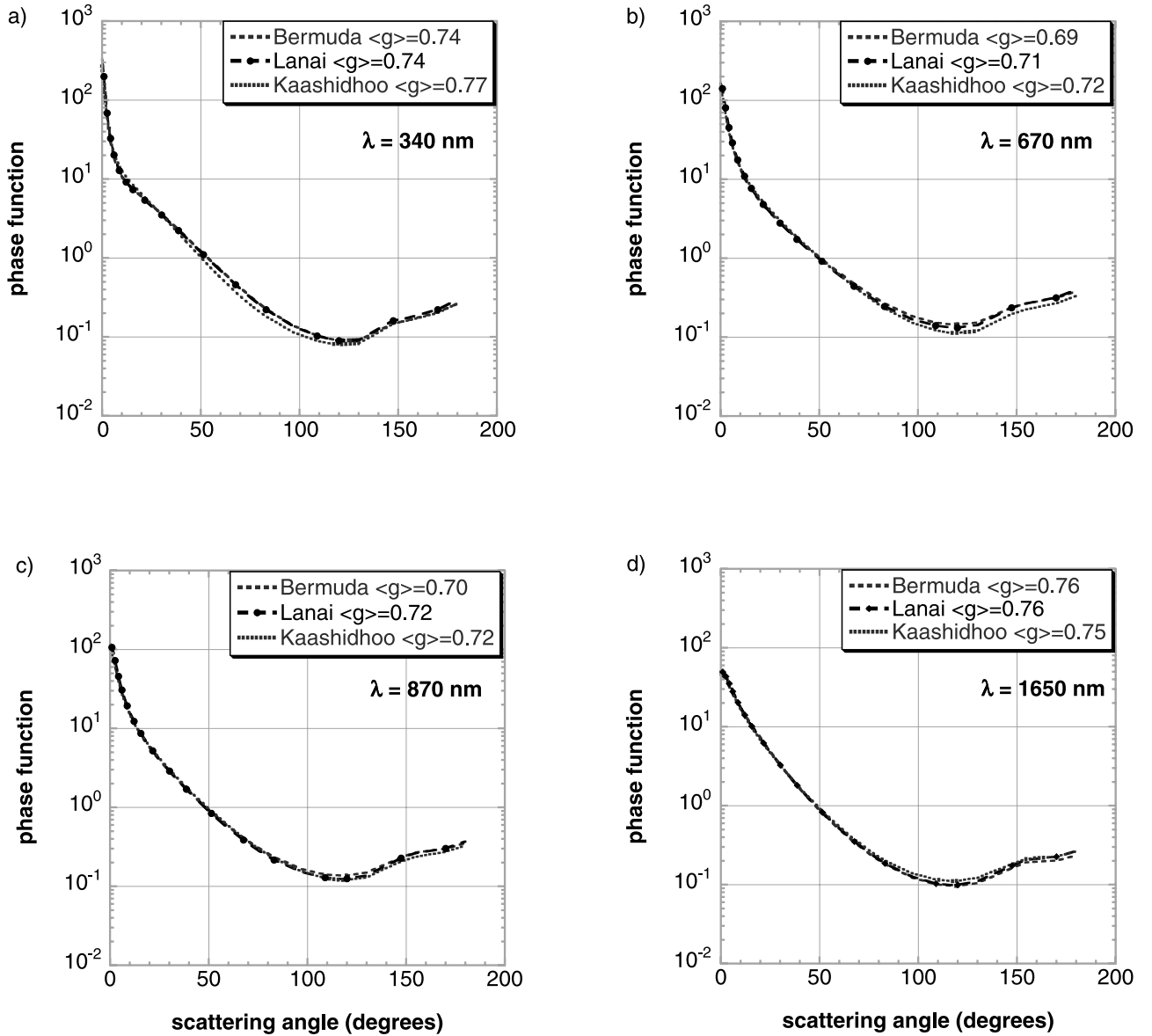
Figure 8. Single-scattering phase functions for various spectral channels ((a) 340 nm, (b) 670 nm, (c) 870 nm, (d) 1650 nm), computed using size distributions from Figure 3 and refractive index of 1.37-0.001i.

the analysis of the ship-borne measurements, *Villevalde et al.* [1994] reported $\Delta\alpha \sim 0.5$, noting that the difference between α_{vis} and α_{nir} illustrates the fact that the coarse mode of the particles is of different origin (sea-spray) and to a certain extent varies independently. Computations of the Angstrom parameter from computed τ_a in the range 440–870 nm (principally as means of comparison with previous results) yielded values 0.65 for Lanai and 0.82 for Bermuda, which are very close to the general statistics presented by *Holben et al.* [2001] and *Smirnov et al.* [2002].

[25] Single-scattering phase functions in the spectral range 340–2130 nm for the averaged Lanai size distribution of Figure 3 and the maritime model refractive index are listed in Table 2. A comparison among the 3 sites for a number of spectral channels is shown in Figures 8a–8d. For various sensors (MODIS, MISR, Sea-WIFS) the realistic

range of scattering angles observed is located between about $60°$ and $160°$degrees. As we can see from Figure 8 the phase functions for Lanai and Bermuda are very close across the whole spectral and angular ranges. The Kaashidhoo phase function differs slightly, although only in the UV and visible spectral ranges.

3. Conclusions

[26] The aerosol model presented in the paper can be employed as a maritime look up table (LUT) kernel in coupled atmospheric retrieval and correction algorithms. It can also be advantageously employed as a LUT inversion kernel in pure aerosol retrieval schemes [*Tanré et al.*, 1997] or in algorithms for the classification of aerosol mixtures [*Kahn et al.*, 1998, 2001]. The maritime aerosol model can

be used as the defining single component of pure maritime air masses or in combination with various aerosol types (dust, biomass burning, etc.). Finally, the model can serve as a source of input to aerosol transport models and radiative forcing simulations.

[27] The model encompasses a variety of maritime conditions in the simplest manner possible. It requires further validation based on the accumulated evidence of microphysical and optical measurements tied to radiative transfer closure experiments. The aerosol model presented in the paper can be tested as a candidate model versus the Shettle-Fenn parameterization in atmospheric correction algorithms. The impact of the model on retrieved water leaving radiances (as part of an atmospheric correction procedure) will be the subject of a separate paper.

References

Badaev, V. V., M. S. Malkevich, B. Pizik, and G. Zimmermann, Determination of the optical parameters of the Earth's surface, of the atmosphere and of the ocean, from the Interkosmos 20 and 21 satellites, *Sov. J. Remote Sens.*, 5(5), 812–834, 1989.

Bates, T. S., V. N. Kapustin, P. K. Quinn, D. S. Covert, D. J. Coffman, C. Mari, P. A. Durkee, W. J. De Bruyn, and E. S. Saltzman, Processes controlling the distribution of aerosol particles in the lower marine boundary layer during the First Aerosol Characterization Experiment (ACE 1), *J. Geophys. Res.*, 103, 16,369–16,383, 1998.

Bates, T. S., P. K. Quinn, D. S. Covert, D. J. Coffman, J. E. Johnson, and A. Wiedensohler, Aerosol physical properties and processes in the lower marine boundary layer: A comparison of shipboard sub-micron data from ACE-1 and ACE-2, *Tellus, Ser. B*, 52, 258–272, 2000.

Brechtel, F. J., S. M. Kreidenweis, and H. B. Swan, Air mass characteristics, aerosol particle number concentrations, and number size distributions at Macquarie Island during the First Aerosol Characterization Experiment (ACE 1), *J. Geophys. Res.*, 103, 16,351–16,367, 1998.

Chomko, R. M., and H. R. Gordon, Atmospheric correction of ocean color imagery: Use of the Junge power-law aerosol size distribution with variable refractive index to handle aerosol absorption, *Appl. Opt.*, 37, 5560–5572, 1998.

Clarke, A. D., W. G. Collins, P. J. Rasch, V. N. Kapustin, K. Moore, S. Howell, and H. E. Fuelberg, Dust and pollution transport on global scales: Aerosol measurements and model predictions, *J. Geophys. Res.*, 106, 32,555–32,569, 2001.

Dubovik, O., and M. D. King, A flexible inversion algorithm for retrieval of aerosol optical properties from sun and sky radiance measurements, *J. Geophys. Res.*, 105, 20,673–20,696, 2000.

Dubovik, O., A. Smirnov, B. N. Holben, M. D. King, Y. J. Kaufman, T. F. Eck, and I. Slutsker, Accuracy assessments of aerosol optical properties retrieved from AERONET sun and sky radiance measurements, *J. Geophys. Res.*, 105, 9791–9806, 2000.

Dubovik, O., B. N. Holben, T. F. Eck, A. Smirnov, Y. J. Kaufman, M. D. King, D. Tanré, and I. Slutsker, Variability of absorption and optical properties of key aerosol types observed in worldwide locations, *J. Atmos. Sci.*, 59, 590–608, 2002.

Eck, T. F., B. N. Holben, J. S. Reid, O. Dubovik, A. Smirnov, N. T. O'Neill, I. Slutsker, and S. Kinne, Wavelength dependence of the optical depth of biomass burning, urban, and desert dust aerosol, *J. Geophys. Res.*, 104, 31,333–31,350, 1999.

Eck, T. F., B. N. Holben, O. Dubovik, A. Smirnov, I. Slutsker, J. M. Lobert, and V. Ramanathan, Column-integrated aerosol optical properties over the Maldives during the northeast monsoon for 1998–2000, *J. Geophys. Res.*, 106, 28,555–28,566, 2001.

Eck, T. F., et al., Variability of biomass burning aerosol optical characteristics in southern Africa during the SAFARI 2000 dry season campaign and a comparison of single scattering albedo estimates from radiometric

measurements, *J. Geophys.*, 108, doi:10.109/2002JD002321, in press, 2003.

Fraser, R. S., S. Mattoo, E.-N. Yeh, and C. R. McClain, Algorithm for atmospheric and glint corrections of satellite measurements of ocean pigment, *J. Geophys. Res.*, 102, 17,107–17,118, 1997.

Gao, B.-C., M. J. Montes, Z. Ahmad, and C. O. Davis, Atmospheric correction algorithm for hyper spectral remote sensing of ocean color from space, *Appl. Opt.*, 39, 887–896, 2000.

Gathman, S. G., Optical properties of the marine aerosol as predicted by the Navy aerosol model, *Opt. Eng.*, 22, 57–62, 1983.

Gordon, H. R., Atmospheric correction of ocean color imagery in the Earth Observing System era, *J. Geophys. Res.*, 102, 17,081–17,106, 1997.

Gordon, H. R., and M. Wang, Retrieval of water-leaving radiance and aerosol optical thickness over the oceans with SeaWiFS: A preliminary algorithm, *Appl. Opt.*, 33, 443–452, 1994.

Gras, J. L., CN, CNN and particle size in Southern Ocean air at Cape Grim, *Atmos. Res.*, 35, 233–251, 1995.

Haywood, J., P. Francis, O. Dubovik, M. D. Glew, and B. N. Holben, Comparison of aerosol size distributions, radiative properties and optical depths determined by aircraft observations and sunphotometers during SAFARI 2000, *J. Geophys.*, 108, doi:10.1029/2002JD002250, in press, 2003.

Hess, M., P. Koepke, and I. Schult, Optical properties of aerosols and clouds: The software package OPAC, *Bull. Am. Meteorol. Soc.*, 79, 831–844, 1998.

Holben, B. N., et al., AERONET: A federated instrument network and data archive for aerosol characterization, *Remote Sens. Environ.*, 66(1), 1–16, 1998.

Holben, B. N., et al., An emerging ground based aerosol climatology: Aerosol optical depth from AERONET, *J. Geophys. Res.*, 106, 12,067–12,097, 2001.

Horvath, H., R. L. Gunter, and S. W. Wilkinson, Determination of the coarse mode of the atmospheric aerosol using data from a forward-scattering spectrometer probe, *Aerosol Sci. Technol.*, 12, 964–980, 1990.

Jennings, S. G., and C. D. O'Dowd, Volatility of aerosol at Mace Head, on the west coast of Ireland, *J. Geophys. Res.*, 95, 13,937–13,948, 1990.

Jennings, S. G., M. Geever, F. M. McGovern, J. Francis, T. G. Spain, and T. Donaghy, Microphysical and physico-chemical characterization of atmospheric marine and continental aerosol at Mace Head, *Atmos. Environ.*, 31, 2795–2808, 1997.

Kahn, R., P. Banerjee, D. McDonald, and D. J. Diner, Sensitivity of multiangle imaging to aerosol optical depth and to pure-particle size distribution and composition over the ocean, *J. Geophys. Res.*, 103, 32,195–32,213, 1998.

Kahn, R., P. Banerjee, and D. McDonald, Sensitivity of multiangle imaging to natural mixtures of aerosols over ocean, *J. Geophys. Res.*, 106, 18,219–18,238, 2001.

Kaufman, Y. J., A. Smirnov, B. N. Holben, and O. Dubovik, Baseline maritime aerosol: methodology to derive the optical thickness and scattering properties, *Geophys. Res. Lett.*, 28, 3251–3254, 2001.

Kim, Y., H. Sievering, and J. Boatman, Volume and surface area size distribution, water mass and model fitting of GCE/CASE/WATOX marine aerosols, *Global Biogeochem. Cycles*, 4, 165–177, 1990.

Kim, Y., H. Sievering, J. Boatman, D. Wellman, and A. Pszenny, Aerosol size distribution and aerosol water content measurements during Atlantic Stratocumulus Transition Experiment/Marine Aerosol and Gas Exchange, *J. Geophys. Res.*, 100, 23,027–23,038, 1995.

O'Dowd, C. D., M. H. Smith, and S. R. Jennings, Submicron particles, radon, and soot carbon characteristics over the Northeast Atlantic, *J. Geophys. Res.*, 98, 1123–1135, 1993.

O'Dowd, C. D., M. H. Smith, I. E. Consterdine, and J. A. Lowe, Marine aerosol, sea-salt, and the marine sulphur cycle: A short review, *Atmos. Environ.*, 31, 73–80, 1997.

Patterson, E. M., C. S. Kiang, A. C. Delany, A. F. Wartburg, A. C. D. Leslie, and B. J. Huebert, Global measurements of aerosols in remote continental and marine regions: Concentrations, size distributions, and optical properties, *J. Geophys. Res.*, 85, 7361–7376, 1980.

Perry, K. D., T. A. Cahill, R. C. Schnell, and J. M. Harris, Long-range transport of anthropogenic aerosols to the National Oceanic and Atmospheric Administration baseline station at Mauna Loa Observatory, Hawaii, *J. Geophys. Res.*, 104, 18,521–18,533, 1999.

Porter, J. N., and A. D. Clarke, Aerosol size distribution models based on in situ measurements, *J. Geophys. Res.*, 102, 6035–6045, 1997.

Pueschel, R. F., J. M. Livingston, G. V. Ferry, and T. E. DeFelice, Aerosol abundances and optical characteristics in the Pacific basin free troposphere, *Atmos. Environ.*, 28, 951–960, 1994.

Quinn, P. K., S. F. Marshall, T. S. Bates, D. S. Covert, and V. N. Kapustin, Comparison of measured and calculated aerosol properties relevant to the direct radiative forcing of tropospheric sulfate aerosol on climate, *J. Geophys. Res.*, 100, 8977–8991, 1995.

Quinn, P. K., V. N. Kapustin, T. S. Bates, and D. S. Covert, Chemical and optical properties of marine boundary layer aerosol particles of the mid-Pacific in relation to sources and meteorological trasport, *J. Geophys. Res.*, *101*, 6931–6951, 1996.

Quinn, P. K., D. J. Coffman, T. S. Bates, T. L. Miller, J. E. Johnson, K. Voss, E. J. Welton, and C. Neususs, Dominant aerosol chemical components and their contribution to extinction during the AEROSL99 cruise across the Atlantic, *J. Geophys. Res.*, *106*, 20,783–20,810, 2001.

Ramanathan, V., et al., The Indian Ocean Experiment: An integrated assessment of the climate forcing and effects of the great Indo-Asian haze, *J. Geophys. Res.*, *106*, 28,371–28,398, 2001.

Reid, J. S., P. V. Hobbs, R. J. Ferek, D. R. Blake, J. V. Martrins, M. R. Dunlap, and C. Liousse, Physical, chemical, and optical properties of regional hazes dominated by smoke in Brazil, *J. Geophys. Res.*, *103*, 32,059–32,080, 1998.

Reid, J. S., H. H. Jonsson, M. H. Smith, and A. Smirnov, Evolution of the vertical profile and flux of large sea-salt particles in a coastal zone, *J. Geophys. Res.*, *106*, 12,039–12,054, 2001.

Reid, J. S., et al., Comparison of size and morphological measurements of coarse mode dust particles from Africa, *J. Geophys.*, *108*, doi:10.1029/2002JD002485, in press, 2003.

Russell, P. B., et al., Pinatubo and pre-Pinatubo optical depth spectra: Mauna Loa measurements, comparisons, inferred particle size distributions, radiative effects, and relationship to lidar data, *J. Geophys. Res.*, *98*, 22,969–22,985, 1993.

Sakerin, S. M., and D. M. Kabanov, Spatial inhomogeneities and the spectral behavior of atmospheric aerosol optical depth over the Atlantic Ocean, *J. Atmos. Sci.*, *59*, 484–500, 2002.

Satheesh, S. K., V. Ramanathan, X. Li-Jones, J. M. Lobert, I. A. Podgorny, J. M. Prospero, B. N. Holben, and N. G. Loeb, A model for the natural and anthropogenic aerosols over the tropical Indian Ocean derived from Indian Ocean Experiment data, *J. Geophys. Res.*, *104*, 27,421–27,440, 1999.

Schwindling, M., P. Y. Deschamps, and R. Frouin, Verification of aerosol models for satellite ocean color remote sensing, *J. Geophys. Res.*, *103*, 24,919–24,935, 1998.

Shaw, G. E., Transport of Asian desert dust to the Hawaiian Islands, *J. Appl. Meteorol.*, *19*, 1254–1259, 1980.

Shettle, E. P., and R. W. Fenn, Models for the aerosols of the lower atmosphere and the effects of humidity variations on their optical properties, *AFGL Tech. Rep., AFGL-TR-79-0214*, 1979.

Smirnov, A., B. N. Holben, T. F. Eck, O. Dubovik, and I. Slutsker, Cloud screening and quality control algorithms for the AERONET data base, *Remote Sens. Environ.*, *73*(3), 337–349, 2000.

Smirnov, A., B. N. Holben, Y. J. Kaufman, O. Dubovik, T. F. Eck, I. Slutsker, C. Pietras, and R. N. Halthore, Optical properties of atmospheric aerosol in maritime environments, *J. Atmos. Sci.*, *59*, 501–523, 2002.

Tanre, D., Y. J. Kaufman, M. Herman, and S. Mattoo, Remote sensing of aerosol properties over oceans using the MODIS/EOS spectral radiances, *J. Geophys. Res.*, *102*, 16,971–16,988, 1997.

Thulasiraman, S., N. T. O'Neill, A. Royer, B. N. Holben, D. L. Westphal, and L. J. B. McArthur, Sunphotometric observations of the 2001 Asian dust storm over Canada and the U.S., *Geophys. Res. Lett.*, *29*(8), 1255, 10.1029/2001GL014188, 2002.

Villevalde, Y. V., A. V. Smirnov, N. T. O'Neill, S. P. Smyshlyaev, and V. V. Yakovlev, Measurement of aerosol optical depth in the Pacific Ocean and the North Atlantic, *J. Geophys. Res.*, *99*, 20,983–20,988, 1994.

Yan, B., K. Stamnes, W. Li, B. Chen, J. J. Stamnes, and S.-C. Tsay, Pitfalls in atmospheric correction of ocean color imagery: how should aerosol optical properties be computed, *Appl. Opt.*, *41*, 412–423, 2002.

———————————

O. Dubovik, T. F. Eck, and A. Smirnov, Goddard Earth Sciences and Technology Center, NASA Goddard Space Flight Center, Code 923, Greenbelt, MD 20771, USA. (dubovik@aeronet.gsfc.nasa.gov; tom@aeronet.gsfc.nasa.gov; asmirnov@aeronet.gsfc.nasa.gov)

R. Frouin, Scripps Institution of Oceanography, University of California, San Diego, 9500 Gilman Drive, La Jolla, CA 92037, USA. (rfrouin@ucsd.edu)

B. N. Holben and I. Slutsker, Biospheric Sciences Branch, NASA Goddard Space Flight Center, Code 923, Greenbelt, MD 20771, USA. (brent@aeronet.gsfc.nasa.gov; ilya@aeronet.gsfc.nasa.gov)